Available online at www.sciencedirect.com
SCIENCE DIRECT®
International Journal of Solids and Structures 42 (2005) 1225–1251
INTERNATIONAL JOURNAL OF SOLIDS and STRUCTURES
www.elsevier.com/locate/ijsolstr

Stability and vibration of shear deformable plates—first order and higher order analyses

I. Shufrin, M. Eisenberger *

Faculty of Civil and Environmental Engineering, Technion Israel Institute of Technology, Rabin Building, Technion City, Haifa 32000, Israel

Received 13 November 2003; received in revised form 17 June 2004
Available online 25 August 2004

Abstract

This work presents the highly accurate numerical calculation of the natural frequencies and buckling loads for thick elastic rectangular plates with various combinations of boundary conditions. The Reissener–Mindlin first order shear deformation plate theory and the higher order shear deformation plate theory of Reddy have been applied to the plate's analysis. The governing equations and the boundary conditions are derived using the dynamic version of the principle of minimum of the total energy. The solution is obtained by the extended Kantorovich method. This approach is combined with the exact element method for the vibration and stability analysis of compressed members, which provides for the derivation of the exact dynamic stiffness matrix including the effect of in-plane and inertia forces. The large number of numerical examples demonstrates the applicability and versatility of the present method. The results obtained by both shear deformation theories are compared with those obtained by the classical thin plate's theory and with published results. Many new results are given too.

Keywords: Extended Kantorovich method; Plate buckling and vibration; First order plate theory; Higher order plate theory; Dynamic stiffness

1. Introduction

Plate elements are commonly used in civil, mechanical, aeronautical and marine structures. The consideration of natural frequencies and buckling loads for rectangular plates are essential to have an efficient and reliable design.

* Corresponding author. Tel.: +972 4 829 3043; fax: +972 4 829 5697.
E-mail address: cvrmosh@tx.technion.ac.il (M. Eisenberger).

0020-7683/$ - see front matter © 2004 Elsevier Ltd. All rights reserved.
doi:10.1016/j.ijsolstr.2004.06.067

The classical Kirchhoff thin plate theory (CPT) is usually used to carry out vibration and stability analysis of rectangular plates. CPT assumptions are satisfactory for low mode computation of truly thin plate, but they can lead to inaccuracy in higher modes calculation or when the ratio of thickness to the dimension of plate is relatively large. This is because the effects of the rotary inertia, which is neglected in most references, and the transverse shear deformations, which cannot be considered in the Kirchhoff theory, become significant in thick plates. Therefore a number of shear deformation plate theories were developed. The simplest one is the first order shear deformation plate theory (FOPT) that is famous as the Reissener–Mindlin theory. This approach extends the kinematic assumptions of the CPT by releasing the restriction on the angle of shearing deformations (Reddy, 1999; Wang et al., 2000). The transverse shear strain is assumed to be constant through the thickness of the plate, and a shear correction factor is introduced to correct the discrepancy between the actual transverse shear stress distribution and those computed using the kinematic relations of this theory. The shear correction factors depend not only on geometric parameters, but also on the loading and boundary conditions of the plate. The application of the Reissner–Mindlin theory to plate problem has attracted the attention of many researchers. Various methods have been applied to compute natural frequencies and buckling loads for thick rectangular plates with different boundary condition, namely the analytical Navier (Reddy and Phan, 1985) and Levy (Liew et al., 1996; Zenkour, 2001) solutions, the Rayleigh–Ritz method (Liew et al., 1995, 1998; Wang et al., 1994; Kitipornchai et al., 1993; Cheung and Zhou, 2000), the finite strip method (Dawe and Roufael, 1982; Roufael and Dawe, 1980; Mizusawa, 1993), the finite difference and finite elements methods etc.

Higher order shear deformation plate theories (HOPT) use higher order polynomials in the expansion of the displacement components through the thickness of the plate. According to the assumptions of HOPT the restriction on warping of the cross section is relaxed, and allows variation in the thickness direction of the plate. Unlike the FOPT, the HOPT requires no shear correction factors. Applications of HOPT for problems of buckling and vibration of thick plates have been discussed by a number of authors. Reddy and Phan (1985) have used the Navier solution in order to analyze the free vibration and buckling of isotropic, orthotropic and laminated rectangular plates with simply supported edge condition according to the HOPT of Reddy (1999). Hanna and Leissa (1994) have developed a completely higher order shear deformation plate theory, including energy functional, equation of motion and boundary condition. They have used Rayleigh–Ritz method for free vibration solution of fully free rectangular plate. Doong (1987) have used the average stress method in order to develop high order plate theory in which an arbitrary initial stress state is included. The governing equations are obtained using a perturbation technique. He has presented the Navier solution for natural frequencies and buckling loads for simply supported rectangular plate. Matsunga (1994) have derived a HOPT through Hamilton's principle by using the method of power series expansion of displacement components. Stability and free vibration analysis have been performed for simply supported plate by Navier method. A broad literature survey on the vibration analysis of shear deformable plates also have been done by Liew et al. (1995).

This work presents the calculation of the natural frequencies and buckling loads for thick elastic rectangular plates with various boundary conditions and includes the effects of shear deformation and rotary inertia. The dynamic version of the principle of minimum of total energy is adopted in derivation of the governing equations and the boundary conditions for Reissener–Mindlin FOPT and HOPT of Reddy. The solution is based on the extended Kantorovich method (Kerr, 1969; Yuan and Jin, 1998; Eisenberger and Alexandrov, 2003). According to this approach solution is assumed to be separable in the directions of plate's edges. Then, the solution in one direction, x for example, is specified a priory, and the solution in the y-direction is determinated by solving an ordinary differential equation derived from the associated variational process with appropriate boundary conditions. In the next step, the obtained solution is used as the known function, while the solution in the second direction is re-determinated by another Kantorovich solution process. These iterations are repeated until the result converges to a desired degree. In the case that two parallel edges are simply supported this procedure yields exact results, as it will be shown. In the solution in

one direction, the exact element method for the vibration and stability analysis of compressed members is used (Eisenberger, 1991, 1995). This approach provides for the derivation of the dynamic stiffness matrix including the effect of in-plane and inertia forces. The desired crucial parameter (buckling load or natural frequency) is found as a value that leads to the singularity of the stiffness matrix. Free vibration and stability of rectangular thick plates are analyzed by varying the plate-aspect ratios and thickness–width ratios. The results obtained by both shear deformation theories (FOPT and HOPT) are compared with those from the classical plate theory (CPT) and with published results. Many new results are given too.

2. Analysis of rectangular plates using shear deformation theories

Consider an isotropic rectangular plate of plan-form L_x and L_y with constant thickness h. The plate has arbitrary boundary condition and is assumed to be subjected to in-plane load for buckling analysis and to inertia forces for vibration analysis. The coordinate system is taken such that the x–y plane coincides with the middle plane of the plate and the origin of the coordinate system is taken at the lower left corner of the plate (see Fig. 1). Note that the in-plane shear forces are not included. As Yuan and Jin (1998) showed, the simplest one term separation of variables, which is used in the current study, does not enable to include in-plane shear force, as these cancel out in the derivation.

3. First order shear deformation plate theory

3.1. Governing equations

According to Reissener–Mindlin theory for harmonic motion the displacement field is taken as

$$\bar{u}(x,y,z,t) = z\overline{\psi}_x(x,y,t) = z\psi_x(x,y)\mathrm{e}^{\mathrm{i}\omega t} \tag{1a}$$

$$\bar{v}(x,y,z,t) = z\overline{\psi}_y(x,y,t) = z\psi_y(x,y)\mathrm{e}^{\mathrm{i}\omega t} \tag{1b}$$

$$\bar{w}(x,y,z,t) = \bar{w}_0(x,y,t) = w_0(x,y)\mathrm{e}^{\mathrm{i}\omega t} \tag{1c}$$

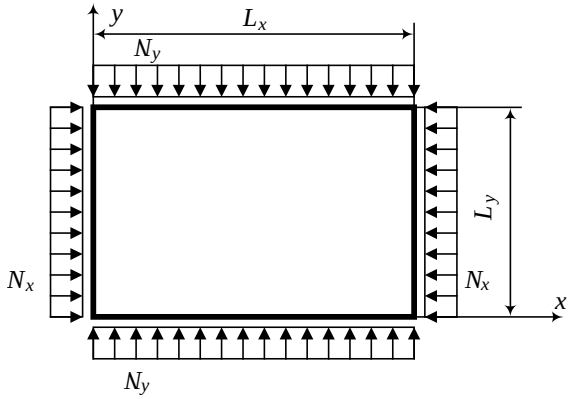

Fig. 1. Geometry and the coordinate system of rectangular plates.

where $(\bar{u}, \bar{v}, \bar{w})$ are the displacement components along the (x, y, z) coordinate directions, respectively; $\bar{w}_0$ is the transverse deflection of a point on the middle plane, ψ_x and ψ_y denote the rotations around to the x- and y-axes, correspondingly, and ω denotes the angular natural frequency.

The out of plane energy functional for rectangular plate Π, associated with the above displacements, can be written in terms of strain energy of bending, kinetic energy of vibration and potential energy of in-plane loads (see Fig. 1) in following form (Reddy, 1999):

$$\begin{aligned}\Pi = \frac{1}{2} + \int\int_A \Bigg\{ & D\left(\frac{\partial \psi_x}{\partial x} + \frac{\partial \psi_y}{\partial y}\right)^2 + \frac{D(1-\nu)}{2}\left(\left(\frac{\partial \psi_x}{\partial y} + \frac{\partial \psi_y}{\partial x}\right)^2 - \frac{1}{4}\frac{\partial \psi_x}{\partial x}\frac{\partial \psi_y}{\partial y}\right) \\ & + kGh\left(\left(\psi_x + \frac{\partial w_0}{\partial x}\right)^2 + \left(\psi_y + \frac{\partial w_0}{\partial y}\right)\right)^2 - \omega^2\rho\left(hw_0^2 + \frac{h^3}{12}\left(\psi_x^2 + \psi_y^2\right)\right) \\ & + N_x\left(\frac{\partial w_0}{\partial x}\right)^2 + N_y\left(\frac{\partial w_0}{\partial y}\right)^2\Bigg\} \mathrm{d}x\,\mathrm{d}y \end{aligned} \tag{2}$$

In which, the shear modulus G is related to Young's modulus E and Poisson's ratio ν by $G = E/2(1+\nu)$, $D = Eh^3/12(1-\nu^2)$ is the bending rigidity of the plate, ρ is the mass density of the plate's material, and k is the shear correction factor to compensate for the discrepancy between the parabolic distribution of transverse shear stresses and the constant state of shear stresses resulting from the kinematic assumptions of this theory.

According to the classical Kantorovich method for 2-D problem we assume that the solution is separable, and can be written as

$$w(x,y) = w(x)W(y) \tag{3a}$$

$$\psi_x(x,y) = f(x)F(y) \tag{3b}$$

$$\psi_y(x,y) = \phi(x)\Phi(y) \tag{3c}$$

Substitution of the assumed solution Eqs. (3a)–(3c) and its derivatives into the energy functional equation (2) yields

$$\begin{aligned}\Pi = & \frac{D}{2}\int_0^{L_x}\int_0^{L_y}\left(f_{,x}^2F^2 + \phi^2\Phi_{,y}^2 + 2f_{,x}\phi\nu F\Phi_{,y} + f^2\frac{1}{2}(1-\nu)F_{,y}^2 + 2f\phi_{,x}\frac{1}{2}(1-\nu)F_{,y}\Phi + \phi_{,x}^2\frac{1}{2}(1-\nu)\Phi^2\right)\mathrm{d}x\,\mathrm{d}y \\ & + \frac{kGh}{2}\int_0^{L_x}\int_0^{L_y}(f^2F^2 + 2fw_{,x}FW + w_{,x}^2W^2 + \phi^2\Phi^2 + \phi w\Phi W_{,y} + w^2W_{,y}^2)\,\mathrm{d}x\,\mathrm{d}y \\ & - \frac{D}{2}\int_0^{L_x}\int_0^{L_y}(\Omega^2h^2f^2F^2 + \Omega^2h^2\phi^2\Phi^2 + \Omega^2w^2W^2 + P_xw_{,x}^2W^2 + P_yw^2W_{,y}^2)\,\mathrm{d}x\,\mathrm{d}y \end{aligned} \tag{4}$$

where $\Omega^2 = \omega^2\rho h/D$ and $P_i = N_i/D$. In order to obtain an equation involving only one function, for example $w(x)$ we assume function $W(y)$ as known, and after integration over the direction y the functional takes the form

$$\begin{aligned}\Pi = & \frac{D}{2}\int_0^{L_x}(S_1f_{,x}^2 + S_2\phi^2 + 2S_3f_{,x}\phi + S_4f^2 + 2S_5f\phi_{,x} + S_6\phi_{,x}^2 + S_7f^2 + 2S_8fw_{,x} + S_9w_{,x}^2 + S_{10}\phi^2 \\ & + 2S_{11}\phi w + S_{12}w^2 - S_{13}\Omega^2f^2 - S_{14}\Omega^2\phi^2 - S_{15}\Omega^2w^2 - S_{15}P_xw_{,x}^2 - S_{16}P_yw^2)\,\mathrm{d}x \end{aligned} \tag{5}$$

where the coefficients S_1–S_{16} are defined as

$$
\begin{aligned}
&S_1 = \int_0^{L_y} F^2\,\mathrm{d}y, \quad S_2 = \int_0^{L_y} \Phi_{,y}^2\,\mathrm{d}y, \quad S_3 = \int_0^{L_y} vF\Phi_{,y}\,\mathrm{d}y,\\
&S_4 = \int_0^{L_y} \frac{1}{2}(1-v)F_{,y}^2\,\mathrm{d}y, \quad S_5 = \int_0^{L_y} \frac{1}{2}(1-v)F_{,y}\Phi\,\mathrm{d}y, \quad S_6 = \int_0^{L_y} \frac{1}{2}(1-v)\Phi^2\,\mathrm{d}y,\\
&S_7 = k\int_0^{L_y} \frac{6(1-v)}{h^2}F^2\,\mathrm{d}y, \quad S_8 = k\int_0^{L_y} \frac{6(1-v)}{h^2}FW\,\mathrm{d}y, \quad S_9 = k\int_0^{L_y} \frac{6(1-v)}{h^2}W^2\,\mathrm{d}y,\\
&S_{10} = k\int_0^{L_y} \frac{6(1-v)}{h^2}\Phi^2\,\mathrm{d}y, \quad S_{11} = k\int_0^{L_y} \frac{6(1-v)}{h^2}\Phi W_{,y}\,\mathrm{d}y, \quad S_{12} = k\int_0^{L_y} \frac{6(1-v)}{h^2}W_{,y}^2\,\mathrm{d}y,\\
&S_{13} = \int_0^{L_y} h^2F^2\,\mathrm{d}y, \quad S_{14} = \int_0^{L_y} h^2\Phi^2, \quad S_{15} = \int_0^{L_y} W^2\,\mathrm{d}y, \quad S_{16} = \int_0^{L_y} W_{,y}^2\,\mathrm{d}y
\end{aligned}
\tag{6}
$$

According to the dynamic version of the principle of virtual displacement, i.e., Hamilton's principle the first variation of the functional should be equal to zero. Thus after integration by parts we get

$$
\begin{aligned}
\delta\Pi = \int_0^{L_x} &(((P_xS_{15} - S_9)w_{,xx} + (S_{12} - \Omega^2S_{15} - P_yS_{16})w - S_8f_{,x} + S_{11}\phi)\delta w\\
&+ (-S_1f_{,xx} + (S_4 + S_7 - \Omega^2S_{13})f + (S_5 - S_3)\phi_{,x} + S_8w_{,x})\delta f + (-S_6\phi_{,xx} + (S_2 + S_{10} - \Omega^2S_{14})\phi\\
&+ (S_3 - S_5)f_{,x} + S_{11}w)\delta\phi)\,\mathrm{d}x + ((S_9 - P_xS_{15})w_{,x} + S_8f)\delta w|_0^{L_x} + (S_1f_{,x} + S_3\phi)\delta f|_0^{L_x}\\
&+ (S_6\phi_{,x} + S_5f)\delta\phi|_0^{L_x} = 0
\end{aligned}
\tag{7}
$$

Each term in the above equation have to be equal to zero. From the first integral we obtain the system of differential equations in the following form:
For δw

$$(P_xS_{15} - S_9)w_{,xx} + (S_{12} - \Omega^2S_{15} - P_yS_{16})w - S_8f_{,x} + S_{11}\phi = 0 \tag{8}$$

For δf

$$-S_1f_{,xx} + (S_4 + S_7 - \Omega^2S_{13})f + (S_5 - S_3)\phi_{,x} + S_8w_{,x} = 0 \tag{9}$$

For $\delta\phi$

$$-S_6\phi_{,xx} + (S_2 + S_{10} - \Omega^2S_{14})\phi + (S_3 - S_5)f_{,x} + S_{11}w = 0 \tag{10}$$

The remaining expressions are the natural boundary conditions:

$$\delta f: \quad M_\mathrm{b} = (S_1f_{,x} + S_3\phi)|_0^{L_x} \tag{11a}$$

$$\delta\phi: \quad M_\mathrm{t} = (S_5\mathrm{d}f + S_6\mathrm{d}\phi_{,x})|_0^{L_x} \tag{11b}$$

$$\delta\phi: \quad M_\mathrm{t} = (S_5f + S_6\phi_{,x})|_0^{L_x} \tag{11c}$$

where Q the shear force, M_b the bending moment and M_t twisting moment on the corresponding edge of the plate.

3.2. The solution

For the solution, we use the following dimensionless coordinates: $\xi = x/L_x$ and $\eta = y/L_y$. Now we assume the solution of the system Eqs. (8)–(10) as three infinite power series of the following form:

$$w = \sum_{i=0}^{\infty} w_i \xi^i \tag{12a}$$

$$f = \sum_{i=0}^{\infty} f_i \xi^i \tag{12b}$$

$$\phi = \sum_{i=0}^{\infty} \phi_i \xi^i \tag{12c}$$

For the solution we have to find the appropriate coefficients of the polynomials in Eqs. (12a)–(12c). Calculating all the derivatives and substituting them back into Eqs. (8)–(10), we obtain recurrence formulas for calculation $w_{i+2}, f_{i+2}, \phi_{i+2}$ in the series Eqs. (12a)–(12c) as a function of the first two terms of the each series (Eisenberger, 1991, 1995;Eisenberger and Alexandrov, 2003):

$$w_{i+2} = \frac{(S_{15} - \Omega^2 S_{15} - S_{16}P_y)L_x^2 w_i - S_8 L_x (i+1) f_{i+1} + S_{11} L_x^2 \phi_i}{(S_9 - P_x S_{15})(i+1)(i+2)} \tag{13a}$$

$$f_{i+2} = \frac{(S_4 + S_7 - S_{13}\Omega^2)L_x^2 f_i + S_8 L_x (i+1) w_{i+1} + (S_5 - S_3) L_x (i+1)\phi_{i+1}}{S_1 (i+1)(i+2)} \tag{13b}$$

$$\phi_{i+2} = \frac{(S_2 + S_{10} - S_{14}\Omega^2)L_x^2 \phi_i + S_{11} L_x^2 w_i + (S_3 - S_5) L_x (i+1) f_{i+1}}{S_6 (i+1)(i+2)} \tag{13c}$$

Then the first two terms of each series should be found using the boundary condition (Eisenberger and Alexandrov, 2003).

Based on the above technique and using the finite element approach, the six basic shapes can be found with the following boundary conditions:

$$w(0) = 1, \quad w(1) = f(0) = f(1) = \phi(0) = \phi(1) = 0 \tag{14a}$$

$$w(1) = 1, \quad w(0) = f(0) = f(1) = \phi(0) = \phi(1) = 0 \tag{14b}$$

$$f(0) = 1, \quad w(0) = w(1) = f(1) = \phi(0) = \phi(1) = 0 \tag{14c}$$

$$f(1) = 1, \quad w(0) = w(1) = f(0) = \phi(0) = \phi(1) = 0 \tag{14d}$$

$$\phi(0) = 1, \quad w(0) = w(1) = f(0) = f(1) = \phi(1) = 0 \tag{14e}$$

$$\phi(1) = 1, \quad w(0) = w(1) = f(0) = f(1) = \phi(0) = 0 \tag{14f}$$

The calculated shapes are the "exact" solution for the system of differential equations. The word "exact" means "as exact as one can get on a digital computer". This is so since the calculation of the series is stopped according to a preset criterion so that the values of last six terms are less than an arbitrary small criterion (in the present work the criterion is taken as 10^{-20}).

The terms of the stiffness matrix are defined as the holding actions at both ends of the strip, due to unit translation or rotations, at each of the six degrees of freedom, one at the time. Then according to condition Eqs. (11a)–(11c), with transformations to the non-dimensional coordinates we have for the columns of the first order stiffness matrix $S_F(i,j)$ the following expressions:

$$S_{\mathrm{F}}(1,i) = S_8 f^{(i)}(0) + S_9 \frac{1}{L_x} w^{(i)}_{,\xi}(0) - P_x S_{15} \frac{1}{L_x} w^{(i)}_{,\xi}(0) \tag{15a}$$

$$S_{\mathrm{F}}(2,i) = S_1 \frac{1}{L_x} f^{(i)}_{,\xi}(0) + S_3 \phi^{(i)}(0) \tag{15b}$$

$$S_{\mathrm{F}}(3,i) = S_5 f^{(i)}(0) + S_6 \frac{1}{L_x} \phi^{(i)}_{,\xi}(0) \tag{15c}$$

$$S_{\mathrm{F}}(4,i) = S_8 f^{(i)}(1) + S_9 \frac{1}{L_x} w^{(i)}_{,\xi}(1) - P_x S_{15} w^{(i)}_{,\xi}(1) \tag{15d}$$

$$S_{\mathrm{F}}(5,i) = S_1 \frac{1}{L_x} f^{(i)}_{,\xi}(1) + S_3 \phi^{(i)}(1) \tag{15e}$$

$$S_{\mathrm{F}}(6,i) = S_5 f^{(i)}(1) + S_6 \frac{1}{L_x} \phi^{(i)}_{,\xi}(1) \tag{15f}$$

where $w^{(i)}$, $f^{(i)}$, $\phi^{(i)}$ are the shapes that are calculated with the boundary conditions of Eqs. (14a)–(14f)).

Then the natural frequency for the plate can be found as the frequency ω that causes the determinant of the corresponding dynamic stiffness matrix to become zero. Also the buckling loads are the in-plane loads, that lead to singularity of the appropriate matrix, with the frequency $\omega = 0$. This is done using a program that converges on the values that satisfy this criterion.

Having the stiffness matrix for the critical factor we can find the functions of the general displacements for this state by the following procedure: The vector of the nodal displacements is an eigenvector of the stiffness matrix, which corresponds to the desired parameter. Thus, the functions of general displacements are calculated by multiplying the basic shapes functions by the nodal displacement, which is appropriate to each of them.

4. Higher order shear deformation plate theory

4.1. Governing equations

The displacements based on the third order shear deformation plate theory of Reddy (1999) are taken as

$$\bar{u}(x,y,z,t) = \left(z\psi_x - \frac{4z^3}{3h^2}\left(\psi_x + \frac{\partial w_0}{\partial x}\right)\right) \mathrm{e}^{\mathrm{i}\omega t} \tag{16a}$$

$$\bar{v}(x,y,z,t) = \left(z\psi_y - \frac{4z^3}{3h^2}\left(\psi_y + \frac{\partial w_0}{\partial y}\right)\right) \mathrm{e}^{\mathrm{i}\omega t} \tag{16b}$$

$$\bar{w}(x,y,z,t) = w_0 \mathrm{e}^{\mathrm{i}\omega t} \tag{16c}$$

The strain energy of the bending of plate in this case is (Reddy, 1999)

$$U=\frac{1}{2}\int_0^{L_y}\int_0^{L_x}\left\{D\left[\frac{68}{105}\left(\frac{\partial\psi_x}{\partial x}\right)^2+\frac{68}{105}\left(\frac{\partial\psi_y}{\partial y}\right)^2+\frac{1}{21}\left(\frac{\partial^2 w_0}{\partial x^2}\right)^2+\frac{1}{21}\left(\frac{\partial^2 w_0}{\partial y^2}\right)^2\right.\right.$$
$$-\frac{32}{105}\frac{\partial\psi_x}{\partial x}\frac{\partial^2 w_0}{\partial x^2}-\frac{32}{105}\frac{\partial\psi_y}{\partial y}\frac{\partial^2 w_0}{\partial y^2}+2\nu\left(\frac{68}{105}\frac{\partial\psi_x}{\partial x}\frac{\partial\psi_y}{\partial y}+\frac{1}{21}\frac{\partial^2 w_0}{\partial y^2}\frac{\partial^2 w_0}{\partial x^2}\right.$$
$$\left.-\frac{16}{105}\frac{\partial\psi_x}{\partial x}\frac{\partial^2 w_0}{\partial y^2}-\frac{16}{105}\frac{\partial\psi_y}{\partial y}\frac{\partial^2 w_0}{\partial x^2}\right)+\frac{(1-\nu)}{2}\left(\frac{68}{105}\left(\frac{\partial\psi_x}{\partial y}\right)^2+\frac{68}{105}\left(\frac{\partial\psi_y}{\partial x}\right)^2\right.$$
$$\left.\left.+\frac{136}{105}\frac{\partial\psi_x}{\partial y}\frac{\partial\psi_y}{\partial x}+\frac{4}{21}\left(\frac{\partial^2 w_0}{\partial x\partial y}\right)^2-\frac{64}{105}\frac{\partial^2 w_0}{\partial x\partial y}\frac{\partial\psi_x}{\partial y}-\frac{64}{105}\frac{\partial^2 w_0}{\partial x\partial y}\frac{\partial\psi_y}{\partial x}\right)\right]$$
$$\left.+\frac{8}{15}Gh\left(\psi_x+\frac{\partial w_0}{\partial x}\right)^2+\frac{8}{15}Gh\left(\psi_y+\frac{\partial w_0}{\partial y}\right)^2\right\}\mathrm{d}x\,\mathrm{d}y \tag{17}$$

After utilization of the Kantorovich solution technique and integration over the y-direction, we obtain

$$U=\frac{D}{2}\int_0^{L_x}\{S_1 f_{,x}^2+S_2\phi^2+S_3 w_{,xx}^2+S_4 w^2-2S_5 f_{,x}w_{,xx}+2S_6\phi w+2S_7 f_{,x}\phi-2S_8 f_{,x}w+2S_9\phi w_{,xx}$$
$$+2S_{10}ww_{,xx}+S_{11}f^2+S_{12}\phi_{,x}^2+2S_{13}f\phi_{,x}+S_{14}w_{,x}^2-2S_{15}w_{,x}f-2S_{16}w_{,x}\phi_{,x}+S_{17}f^2$$
$$+2S_{18}fw_{,x}+S_{19}w_{,x}^2+S_{20}\phi^2+2S_{21}\phi w+S_{22}w^2\}\,\mathrm{d}x \tag{18}$$

where the S-coefficients are defined as

$$S_1=\frac{68}{105}\int_0^{L_y}F^2\,\mathrm{d}y,\quad S_2=\frac{68}{105}\int_0^{L_y}\Phi_{,y}^2\,\mathrm{d}y,\quad S_3=\frac{1}{21}\int_0^{L_y}W^2\,\mathrm{d}y,$$
$$S_4=\frac{1}{21}\int_0^{L_y}W_{,yy}^2\,\mathrm{d}y,\quad S_5=\frac{16}{105}\int_0^{L_y}FW\,\mathrm{d}y,\quad S_6=-\frac{16}{105}\int_0^{L_y}\Phi_{,y}W_{,yy}\,\mathrm{d}y,$$
$$S_7=\frac{68}{105}\nu\int_0^{L_y}F\Phi_{,y}\,\mathrm{d}y,\quad S_8=\frac{16}{105}\nu\int_0^{L_y}FW_{,yy}\,\mathrm{d}y,\quad S_9=-\frac{16}{105}\nu\int_0^{L_y}\Phi_{,y}W\,\mathrm{d}y,$$
$$S_{10}=\frac{1}{21}\nu\int_0^{L_y}WW_{,yy}\,\mathrm{d}y,\quad S_{11}=\frac{34}{105}(1-\nu)\int_0^{L_y}F_{,y}^2\,\mathrm{d}y,\quad S_{12}=\frac{34}{105}(1-\nu)\int_0^{L_y}\Phi^2\,\mathrm{d}y,$$
$$S_{13}=\frac{34}{105}(1-\nu)\int_0^{L_y}F_{,y}\Phi\,\mathrm{d}y,\quad S_{14}=\frac{2(1-\nu)}{21}\int_0^{L_y}W_{,y}^2\,\mathrm{d}y,\quad S_{15}=\frac{16}{105}(1-\nu)\int_0^{L_y}F_{,y}W\,\mathrm{d}y,$$
$$S_{16}=\frac{16}{105}(1-\nu)\int_0^{L_y}\Phi W\,\mathrm{d}y,\quad S_{17}=\frac{16(1-\nu)}{5h^2}\int_0^{L_y}F^2\,\mathrm{d}y,\quad S_{18}=\frac{16(1-\nu)}{5h^2}\int_0^{L_y}FW\,\mathrm{d}y,$$
$$S_{19}=\frac{16(1-\nu)}{5h^2}\int_0^{L_y}W^2\,\mathrm{d}y,\quad S_{20}=\frac{16(1-\nu)}{5h^2}\int_0^{L_y}\Phi^2\,\mathrm{d}y,\quad S_{21}=\frac{16(1-\nu)}{5h^2}\int_0^{L_y}\Phi W_{,y}\,\mathrm{d}y,$$
$$S_{22}=\frac{16(1-\nu)}{5h^2}\int_0^{L_y}W_{,y}^2\,\mathrm{d}y \tag{19}$$

The assumed free vibration is harmonic and based on the displacement field (Eqs. (16a)–(16c)) we get the expression of kinetic energy in the form

$$T = \omega^2 \frac{\rho}{2} \int\int_A \left[\frac{17}{315} h^3 \psi_x^2 + \frac{17}{315} h^3 \psi_y^2 + \frac{8}{315} h^3 \psi_x \frac{\partial w_0}{\partial x} + \frac{8}{315} h^3 \psi_y \frac{\partial w_0}{\partial y} + h w_0^2 + \frac{h^3}{252} \left(\frac{\partial w_0}{\partial x} \right)^2 + \frac{h^3}{252} \left(\frac{\partial w_0}{\partial y} \right)^2 \right] \mathrm{d}x\,\mathrm{d}y \tag{20}$$

After separation and integration over y-direction it takes the following form:

$$T = \Omega^2 \frac{D}{2} \int_0^{L_x} \{ S_{23} f^2 + S_{24} \phi^2 + 2 S_{25} f w_{,x} + 2 S_{26} \phi w + S_{27} w^2 + S_{28} w_{,x}^2 + S_{29} w^2 \} \mathrm{d}x \tag{21}$$

where $S_{23}, \ldots, S_{29}$ are

$$S_{23} = \frac{17}{315} \int_0^{L_y} h^2 F^2 \mathrm{d}y, \quad S_{24} = \frac{17}{315} \int_0^{L_y} h^2 \Phi^2 \mathrm{d}y, \quad S_{25} = \frac{4}{315} \int_0^{L_y} h^2 F W \mathrm{d}y, \quad S_{26} = \frac{4}{315} \int_0^{L_y} h^2 \Phi W_{,y} \mathrm{d}y,$$
$$S_{27} = \int_0^{L_y} W^2 \mathrm{d}y, \quad S_{28} = \frac{1}{252} \int_0^{L_y} h^2 W^2 \mathrm{d}y, \quad S_{29} = \frac{1}{252} \int_0^{L_y} h^2 W_{,y}^2 \mathrm{d}y \tag{22}$$

The potential energy of the in-plane forces after substituting of the assumed solution and the integration over the y-direction takes the following form:

$$V = \frac{D}{2} \int_0^{L_x} (-S_{30} P_x w_{,x}^2 + S_{31} P_y w^2) \mathrm{d}x \tag{23}$$

where S-coefficients are defined as

$$S_{30} = \int_0^{L_y} W^2 \mathrm{d}y, \quad S_{31} = -\int_0^{L_y} W_{,y}^2 \mathrm{d}y \tag{24}$$

According to Hamilton's principle the first variation of the functional should be equal to zero

$$\delta \Pi = \delta U - \delta T + \delta V = 0 \tag{25}$$

After integrating the expression of virtual energy by parts and collecting the coefficients of δw, δf and $\delta \phi$ we obtain the equations of motion for the strip element:
For δw

$$S_3 w_{,xxx} + (2S_{10} - S_{14} - S_{19} + S_{28}\Omega^2 + S_{30} P_x) w_{,xx} + (S_4 + S_{22} + (S_{27} + S_{29})\Omega^2 + S_{31} P_y) w - S_5 f_{,xxx} - (S_8 - S_{15} + S_{18} - S_{25}\Omega^2) f_{,x} + (S_9 + S_{16}) \phi_{,xx} + (S_6 + S_{21} + S_{26}\Omega^2) \phi) = 0 \tag{26}$$

For δf

$$(S_5 w_{,xxx} + (S_8 - S_{15} + S_{18} - S_{25}\Omega^2) w_{,x} - S_1 f_{,xx} + (S_{11} + S_{17} + S_{23}\Omega^2) f + (S_{13} - S_7) \phi_{,x}) = 0 \tag{27}$$

For $\delta \phi$

$$((S_9 + S_{16}) w_{,xx} + (S_6 + S_{21} + S_{26}\Omega^2) w + (S_7 - S_{13}) f_{,x} - S_{12} \phi_{,xx} + (S_2 + S_{20} + S_{24}\Omega^2) \phi) = 0 \tag{28}$$

The natural boundary conditions (action at the ends of strip elements) are obtained as

$$\delta w\text{: } Q = -\big(S_3 w_{,xxx} + (S_{10} - S_{14} - S_{19} + S_{28}\Omega^2 + S_{31} P_y) w_{,x} - S_5 f_{,xx} + (S_{15} - S_{18} + S_{25}\Omega^2) f + (S_9 + S_{16}) \phi_{,x} \big) \Big|_0^{L_x} \tag{29a}$$

$$\delta w_{,x}\text{: } R = (S_3 w_{,xx} + S_{10} w - S_5 f_{,x} + S_9 \phi) \Big|_0^{L_x} \tag{29b}$$

$$\delta f\colon M_{\mathrm{b}} = (-S_5 w_{,xx} - S_8 w + S_1 f_{,x} + S_7 \phi)|_0^{L_x} \tag{29c}$$

$$\delta \phi\colon M_{\mathrm{t}} = (S_{12}\phi_{,x} + S_{13} f - S_{16} w_{,x})|_0^{L_x} \tag{29d}$$

4.2. The solution

We again use the dimensionless variables ξ and η and the assumption of polynomial variation of all the functions over the strip, Eqs. (12a)–(12c). Now by substitution the assumed solutions, Eqs. (12a)–(12c) into the field equation, Eqs. (26)–(28) we get recurrence formulas for the polynomial terms. All polynomial coefficients dependent on the first four terms of w and the first two of f and ϕ. In contrast with the FOPT analysis, when unknown polynomial terms could be found one after another, in the current HOPT formulation the follow algorithm should be used to calculate them.

Firstly, the f_2 term is calculated for $i = 0$ from the following expressionf:

$$f_2 = \frac{1}{2S_1 L_x}(6S_5 w_3 + L_x^2(S_8 - S_{15} + S_{18} - S_{25}\Omega^2)w_1 + L_x^3(S_{11} + S_{17} + S_{23}\Omega^2)f_0 + (S_{13} - S_7)L_x^2\phi_1) \tag{30}$$

Then for $i = 0,\ldots,\infty$, the ϕ_{i+2} terms are determinated by

$$\begin{aligned}\phi_{i+2} = \frac{1}{S_{12}(i+2)(i+1)}&((S_9 + S_{16})w_{i+2}(i+2)(i+1) + L_x^2(S_6 + S_{21} + S_{26}\Omega^2)w_i \\ &+ L_x(S_7 - S_{13})f_{i+1}(i+1) + L_x^2(S_2 + S_{20} + S_{24}\Omega^2)\phi_i)\end{aligned} \tag{31}$$

Now the terms w_{i+4} and f_{i+3} can be found from the system of two equations:

$$\begin{cases} A_{1,1}^{(i)} w_{i+4} + A_{1,2}^{(i)} f_{i+3} = B_1^{(i)} \\ A_{2,1}^{(i+1)} w_{i+4} + A_{2,2}^{(i+1)} f_{i+3} = B_2^{(i)} \end{cases} \tag{32}$$

where the terms A and B are defined by following expressions:

$$\begin{aligned} A_{1,1}^{(i)} &= -S_3(i+4)(i+3)(i+2)(i+1) \\ A_{1,2}^{(i)} &= S_5 L_x(i+3)(i+2)(i+1) \\ A_{2,1}^{(i)} &= -S_5(i+3)(i+2)(i+1) \\ A_{2,2}^{(i)} &= S_1 L_x(i+2)(i+1) \end{aligned} \tag{33a}$$

$$\begin{aligned} B_1^{(i)} = {} & S_3 w_{i+4}(i+4)(i+3)(i+2)(i+1) + L_x^2(2S_{10} - S_{14} - S_{19} + S_{28}\Omega^2 + S_{30}P_x)w_{i+2}(i+2)(i+1) \\ & + L_x^4(S_4 + S_{22} + (S_{27} + S_{29})\Omega^2 + S_{31}P_y)w_i + L_x^3(-S_8 + S_{15} - S_{18} + S_{25}\Omega^2)f_{i+1}(i+1) \\ & + L_x^2(S_9 + S_{16})\phi_{i+2}(i+2)(i+1) + L_x^4(S_6 + S_{21} + S_{26}\Omega^2)\phi_i \end{aligned} \tag{33b}$$

$$\begin{aligned} B_2^{(i)} = {} & S_5 w_{i+3}(i+3)(i+2)(i+1) + L_x^2(S_8 - S_{15} + S_{18} - S_{25}\Omega^2)w_{i+1}(i+1) + L_x^3(S_{11} + S_{17} + S_{23}\Omega^2)f_i \\ & + L_x^2(S_{13} - S_7)\phi_{i+1}(i+1) \end{aligned} \tag{33c}$$

Then the first four terms of w and the first two of f and ϕ should be found based on boundary conditions. For the current formulation the degrees of freedom are lateral displacement, its derivative and two rotations around the x- and y-axes at both the ends of the strip element. The terms of the stiffness matrix are the holding actions at the end of the strip element due to unit displacement in the desired direction when all other degrees of freedom are restrained. Then for the current formulation the holding end actions are

shear force, twisting moment, ordinary and high order bending moments. Thus, according to conditions of Eqs. (29a)–(29d), with transformation to dimensionless coordinates we have the terms of the higher order stiffness matrix $S_H(i,j)$ as follows:

$$S_{\mathrm{H}}(1,i) = -\frac{1}{L_x^3 S_3} w^{(i)}_{,\xi\xi\xi}(0) - \frac{1}{L_x}(S_{10} - S_{14} - S_{19} + S_{28}\Omega^2 + S_{30}P_x) w^{(i)}_{,\xi}(0) + \frac{1}{L_x^2} S_5 f^{(i)}_{,\xi\xi}(0) - (S_{15} - S_{18} + S_{25}\Omega^2) f^{(i)}(0) - \frac{1}{L_x}(S_9 + S_{16}) \phi^{(i)}_{,\xi}(0) \tag{34a}$$

$$S_{\mathrm{H}}(2,i) = \frac{1}{L_x^2} S_3 w^{(i)}_{,\xi\xi}(0) - \frac{1}{L_x} S_5 f^{(i)}_{,\xi}(0) + S_9 \phi^{(i)}(0) + S_{10} w^{(i)}(0) \tag{34b}$$

$$S_{\mathrm{H}}(3,i) = \frac{1}{L_x} S_1 f^{(i)}_{,\xi}(0) - \frac{1}{L_x^2} S_5 w^{(i)}_{,\xi\xi}(0) + S_7 \phi^{(i)}(0) - S_8 w^{(i)}(0) \tag{34c}$$

$$S_{\mathrm{H}}(4,i) = \frac{1}{L_x} S_{12} \phi^{(i)}_{,\xi}(0) + S_{13} f^{(i)}(0) - \frac{1}{L_x} S_{16} w^{(i)}_{,\xi} \tag{34d}$$

Table 1
Frequency factor λ for SSSS

L_x/L_y	Theory	h/L_y	Mode								
			1,1	2,1	3,1	1,2	2,2	3,2	1,3	2,3	3,3
1	CPT	–	2.0000	5.0000	10.0000	5.0000	8.0000	13.0000	10.0000	13.0000	18.0000
	FOPT	0.1	1.9317	4.6084	8.6162	4.6084	7.0716	10.8093	8.6162	10.8093	14.1908
		0.2	1.7679	3.8656	6.6006	3.8656	5.5879	7.9737	6.6006	7.9737	9.9802
		0.3	1.5768	3.1962	5.1426	3.1962	4.4356	6.0836	5.1426	6.0836	7.4342
		0.4	1.3970	2.6771	4.1505	2.6771	3.6199	4.8521	4.1505	4.8521	5.8537
	HOPT	0.1	1.9317	4.6088	8.6188	4.6088	7.0732	10.8145	8.6188	10.8145	14.2022
		0.2	1.7683	3.8693	6.6176	3.8693	5.5984	8.0030	6.6176	8.0030	10.0362
		0.3	1.5780	3.2059	5.1807	3.2059	4.4605	6.1456	5.1807	6.1456	7.5452
		0.4	1.3996	2.6942	4.2116	2.6942	3.6609	4.9482	4.2116	4.9482	6.0192
1.5	CPT	–	1.4444	2.7778	5.0000	4.4444	5.7778	8.0000	9.4444	10.7778	13.0000
	FOPT	0.1	1.4082	2.6491	4.6084	4.1303	5.2656	7.0716	8.1942	9.1982	10.8093
		0.2	1.3164	2.3612	3.8656	3.5117	4.3405	5.5879	6.3282	6.9717	7.9737
		0.3	1.2010	2.0526	3.1962	2.9336	3.5439	4.4356	4.9536	5.3986	6.0836
		0.4	1.0851	1.7818	2.6771	2.4742	2.9436	3.6199	4.0090	4.3419	4.8521
	HOPT	0.1	1.4082	2.6491	4.6088	4.1306	5.2662	7.0732	8.1965	9.2015	10.8145
		0.2	1.3166	2.3620	3.8693	3.5145	4.3457	5.5984	6.3433	6.9917	8.0030
		0.3	1.2016	2.0553	3.2059	2.9412	3.5569	4.4605	4.9879	5.4425	6.1456
		0.4	1.0864	1.7871	2.6942	2.4879	2.9662	3.6609	4.0643	4.4115	4.9482
2	CPT	–	1.2500	2.0000	3.2500	4.2500	5.0000	6.2500	9.2500	10.0000	11.2500
	FOPT	0.1	1.2227	1.9317	3.0762	3.9611	4.6084	5.6580	8.0453	8.6162	9.5468
		0.2	1.1521	1.7679	2.7023	3.3847	3.8656	4.6183	6.2313	6.6006	7.1916
		0.3	1.0608	1.5768	2.3188	2.8385	3.1962	3.7449	4.8862	5.1426	5.5497
		0.4	0.9664	1.3970	1.9934	2.4004	2.6771	3.0969	3.9585	4.1505	4.4546
	HOPT	0.1	1.2227	1.9317	3.0763	3.9614	4.6088	5.6588	8.0475	8.6188	9.5505
		0.2	1.1522	1.7683	2.7036	3.3872	3.8693	4.6244	6.2457	6.6176	7.2134
		0.3	1.0612	1.5780	2.3227	2.8454	3.2059	3.7602	4.9191	5.1807	5.5972
		0.4	0.9673	1.3996	2.0008	2.4130	2.6942	3.1230	4.0118	4.2116	4.5302

$$S(5,i) = -\frac{1}{L_x^3}S_3 w^{(i)}_{,\xi\xi\xi}(1) - \frac{1}{L_x}(S_{10} - S_{14} - S_{19} + S_{28}\Omega^2 + S_{30}P_x)w^{(i)}_{,\xi}(1) + \frac{1}{L_x^2}S_5 f^{(i)}_{,\xi\xi}(1) - (S_{15} - S_{18} + S_{25}\Omega^2)f^{(i)}(1) - \frac{1}{L_x}(S_9 + S_{16})\phi^{(i)}_{,\xi}(1) \tag{34e}$$

$$S(6,i) = \frac{1}{L_x^2}S_3 w^{(i)}_{,\xi\xi}(1) - \frac{1}{L_x}S_5 f^{(i)}_{,\xi}(1) + S_9\phi^{(i)}(1) + S_{10}w^{(i)}(1) \tag{34f}$$

$$S_{\mathrm{H}}(7,i) = \frac{1}{L_x}S_1 f^{(i)}_{,\xi}(1) - \frac{1}{L_x^2}S_5 w^{(i)}_{,\xi\xi}(1) + S_7\phi^{(i)}(1) - S_8 w^{(i)}(1) \tag{34g}$$

$$S_{\mathrm{H}}(8,i) = \frac{1}{L_x}S_{12}\phi^{(i)}_{,\xi}(1) + S_{13}f^{(i)}(1) - \frac{1}{L_x}S_{16}w^{(i)}_{,\xi} \tag{34h}$$

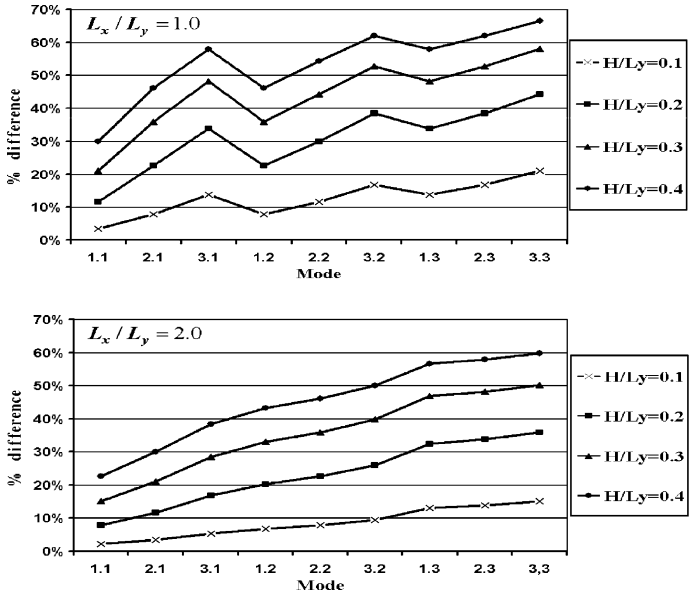

Fig. 2. Comparison of normalized frequency for SSSS plates: % difference CPT to HOPT.

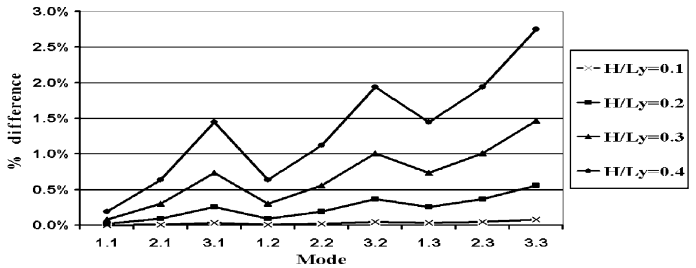

Fig. 3. Comparison of normalized frequency for SSSS plates: % difference FOPT to HOPT, $L_x/L_y = 1.0$.

where $w^{(i)}$, $f^{(i)}$ and $\phi^{(i)}$ are the shapes calculated as the solution of the system of the differential equations of motion, Eqs. (26)–(28) according to the above recurrence technique with the following boundary conditions:

$$w(0) = 1, \quad w(1) = w_{,\xi}(0) = w_{,\xi}(1) = f(0) = f(1) = \phi(0) = \phi(1) = 0 \tag{35a}$$

$$w(1) = 1, \quad w(0) = w_{,\xi}(0) = w_{,\xi}(1) = f(0) = f(1) = \phi(0) = \phi(1) = 0 \tag{35b}$$

$$w_{,\xi}(0) = L_x, \quad w(0) = w(1) = w_{,\xi}(1) = f(1) = f(0) = \phi(0) = \phi(1) = 0 \tag{35c}$$

Table 2
Comparison of the frequency factors λ for SSSS plates ($k = 0.82305$)

L_x/L_y	Theory	Work	h/L_y	Mode								
				1,1	2,1	3,1	1,2	2,2	3,2	1,3	2,3	3,3
1	FOPT	Present	0.1	1.9311	4.6050	8.6054	4.6050	7.0642	10.7932	8.6054	10.7932	14.1647
		Reddy and Phan (1985)		1.9311	4.6077	8.6153	4.6077	7.0724	10.8101	8.6153	10.8101	14.1906
		Liew et al. (1993b)		1.9311	4.6050	8.6055	4.6050	7.0642	10.7932	8.6055	10.7932	–
		Present	0.2	1.7661	3.858	6.582	3.858	5.5737	7.9485	6.582	7.9485	9.9444
		Liew et al. (1993b)		1.7661	3.858	6.582	3.858	5.5737	7.9485	6.582	7.9485	–
	HOPT	Present	0.1	1.9317	4.6088	8.6188	4.6088	7.0732	10.8145	8.6188	10.8145	14.2022
		Reddy and Phan (1985)		1.9332	4.6139	8.6339	4.6139	7.0828	10.8412	8.6339	10.8412	14.2487
		Matsunga (1994)		1.9353	4.6222	8.6609	4.6222	7.1036	10.8786	8.6609	10.8786	14.3048
	3-D solution	Liew et al. (1993a)		1.9342	4.6222	8.6617	4.6222	7.103	10.879	8.6617	10.879	
	HOPT	Present	0.2	1.7683	3.8693	6.6176	3.8693	5.5984	8.003	6.6176	8.003	10.0362
		Matsunga (1994)		1.7759	3.8991	6.6867	3.8991	5.6527	8.0925	6.6867	8.0925	10.1524
	3-D solution	Liew et al. (1993a)		1.7758	3.8991	6.6868	3.8991	5.6524	–	6.6868	–	–
1.5	FOPT	Present	0.1	1.4079	2.6479	4.605	4.1275	5.2613	7.06422	8.1845	9.1862	10.7932
		Liew et al. (1993b)		1.4079	2.6479	4.605	4.1276	5.2613	7.0642	8.1845	–	–
		Present	0.2	1.3153	2.358	3.858	3.5053	4.3313	5.5737	6.3108	6.9514	7.9485
		Liew et al. (1993b)		1.3153	2.358	3.8581	3.5053	4.3313	5.5734	6.3108	–	–
	HOPT	Present	0.1	1.4082	2.6491	4.6088	4.1306	5.2662	7.0732	8.1965	9.2015	10.8145
	3-D solution	Liew et al. (1993a)		1.4096	2.6538		4.1415	5.2834				
	HOPT	Present	0.2	1.3166	2.362	3.8693	3.5145	4.3457	5.5984	6.3432	6.9917	8.003
	3-D solution	Liew et al. (1993a)		1.3209	2.3747		3.5398	4.3489				
	HOPT	Present	0.3	1.2016	2.0553	3.2059	2.9412	3.5569	4.4605	4.9879	5.4425	6.1456
	3-D solution	Liew et al. (1993a)		1.2088	2.0731		2.9719	3.5967				
	HOPT	Present	0.4	1.0864	1.7871	2.6942	2.4879	2.9662	3.6609	4.0643	4.4115	4.9482
	3-D solution	Liew et al. (1993a)		1.0954	1.8064		2.5168	2.9998				

$$w_{,\xi}(1) = L_x, \quad w(0) = w(1) = w_{,\xi}(0) = f(1) = f(0) = \phi(0) = \phi(1) = 0 \tag{35d}$$

$$f(0) = 1, \quad w(0) = w(1) = w_{,\xi}(0) = w_{,\xi}(1) = f(1) = \phi(0) = \phi(1) = 0 \tag{35e}$$

$$f(1) = 1, \quad w(0) = w(1) = w_{,\xi}(0) = w_{,\xi}(1) = f(0) = \phi(0) = \phi(1) = 0 \tag{35f}$$

$$\phi(0) = 1, \quad w(0) = w(1) = w_{,\xi}(0) = w_{,\xi}(1) = f(0) = f(1) = \phi(1) = 0 \tag{35g}$$

$$\phi(1) = 1, \quad w(0) = w(1) = w_{,\xi}(0) = w_{,\xi}(1) = f(0) = f(1) = \phi(0) = 0 \tag{35h}$$

Now the desired critical factor (buckling load or natural frequency) can be found as the value that causes the singularity of the appropriate stiffness matrix. And corresponding to this factor the general displacements can be determinated by the way described for FOPT analysis.

5. Numerical examples

In order to obtain a high precision solution for stability and vibration problems of thick rectangular plates and simultaneously demonstrate the applicability and versatility of the present method, numerical calculations have been performed for a large number of plates with different length–width ratios, thickness–width ratios, and various combinations of boundary conditions.

Table 3
Comparison of the frequency factors λ for SSFF plates ($k = 0.82305$)

L_x/L_y	Theory	Work	h/L_y	Modes							
				1,1	2,1	3,1	1,2	2,2	3,2	1,3	2,3
1	FOPT	Present	0.1	0.9564	3.6815	7.7557	1.5587	4.3327	8.3396	3.4289	6.2908
		Liew et al. (1993b)		0.9564	3.6815	7.7558	1.5588	4.3329	–	3.4290	6.2910
		Present	0.2	0.9096	3.1630	6.0244	1.4267	3.6368	6.3930	2.9482	5.0107
		Liew et al. (1993b)		0.9096	3.1630	6.0245	1.4267	3.6369	–	2.9482	5.0107
	HOPT	Present	0.1	0.9566	3.6841	7.7668	1.5595	4.3366	8.3530	3.4315	6.2990
	3-D solution	Liew et al. (1993a)		0.9571	3.6919		1.5603	4.3454		3.4361	
	HOPT	Present	0.2	0.9103	3.1706	6.0540	1.4287	3.6475	6.4271	2.9547	5.0311
	3-D solution	Liew et al. (1993a)		0.9120	3.1888		1.4309	3.6651		2.9650	
	HOPT	Present	0.3	0.8493	2.6792	4.7826	1.2824	3.0323	5.0428	2.5050	4.0342
	3-D solution	Liew et al. (1993a)		0.8523	2.7010		1.2855	3.0500		2.5168	
	HOPT	Present	0.4	0.7842	2.2821	3.9077	1.1436	2.5549	4.1046	2.1368	3.3130
	3-D solution	Liew et al. (1993a)		0.7883	2.3019		1.1466	2.5665		2.1469	
2	FOPT	Present	0.1	0.2395	0.9564	2.1210	0.6701	1.5587	2.7748	2.5304	3.4289
		Liew et al. (1993b)		0.2395	0.9564	2.1210	0.6701	1.5588	2.7550	2.5304	3.4290
		Present	0.2	0.2362	0.9096	1.9216	0.6310	1.4267	2.4388	2.2614	2.9482
		Liew et al. (1993b)		0.2362	0.9096	1.9216	0.6310	1.4267	2.4388	2.2614	2.9482
	HOPT	Present	0.1	0.2395	0.9566	2.1218	0.6704	1.5595	2.7767	2.5315	3.4315
	3-D solution	Liew et al. (1993a)		0.2396	0.9571		0.6704	1.5603		2.5338	
	HOPT	Present	0.2	0.2362	0.9103	1.9244	0.6317	1.4287	2.4438	2.2644	2.9547
	3-D solution	Liew et al. (1993a)		0.2363	0.9120		0.6319	1.4309		2.2705	
	HOPT	Present	0.3	0.2313	0.8493	1.7033	0.5862	1.2824	2.1085	1.9844	2.5050
	3-D solution	Liew et al. (1993a)		0.2315	0.8523		0.5866	1.2855			
	HOPT	Present	0.4	0.2251	0.7842	1.5014	0.5386	1.1436	1.8230	1.7383	2.1368
	3-D solution	Liew et al. (1993a)		0.2255	0.7883		0.5389	1.1466			

In the previous applications of the extended Kantorovich method for classical thin plate theory (Eisenberger and Alexandrov, 2003) it has been shown that the initial assumed function is neither required to satisfy the essential boundary conditions nor the natural boundary conditions and the quality of the assumption influences only on the number of iterations. According to the present formulations of the two higher order shear deformation theories the solution is the set of the dependent functions of the displacements. Therefore, in order to obtain correct relations between the assumed functions, so that they may satisfy any boundary conditions, the initial displacements are chosen as the lateral deflections and bending rotations of a Timoshenko and high order beams (Eisenberger, 2003), taken from the appropriate direction of the plate as a unit width strip. Although the beam's shapes are not always congruent with the plate's displacement, the iteration convergence proves to be extremely fast. For most cases, only one to two cycles of the iterations are required to produce almost convergent result. The subsequent iterations only serve for more precious determination of the trailing digits. In the present work, the maximal tolerance for the relative error between the iteration steps is taken as 0.0001%. Unlike most of the other numerical methods, in which a better result is obtained by increasing of number of unknowns, the solution in the extended Kantorovich method is improved by continuous enhancement of the operator between successive iteration steps, without additional unknowns.

Table 4
Frequency factor λ for CCCC plates

L_x/L_y	Theory	h/L_y	Mode								
			1,1	2,1	3,1	1,2	2,2	3,2	1,3	2,3	3,3
1	CPT	–	3.6475	7.4375	13.3645	7.4375	10.9666	16.7203	13.3645	16.7203	22.2966
	FOPT	0.1	3.2978	6.2877	10.4299	6.2877	8.8127	12.5568	10.4299	12.5568	15.8491
		0.2	2.6889	4.6915	7.2270	4.6915	6.2994	8.5174	7.2270	8.5174	10.4108
		0.3	2.1733	3.5862	5.3546	3.5862	4.7292	6.2578	5.3546	6.2578	7.5534
		0.4	1.7897	2.8592	4.2192	2.8592	3.7435	4.9019	4.2192	4.9019	5.8833
	HOPT	0.1	3.3046	6.3123	10.4946	6.3123	8.8594	12.6471	10.4946	12.6471	15.9858
		0.2	2.7171	4.7751	7.4078	4.7751	6.4343	8.7458	7.4078	8.7458	10.7264
		0.3	2.2244	3.7175	5.6084	3.7175	4.9270	6.5734	5.6084	6.5734	7.9742
		0.4	1.8598	3.0206	4.5130	3.0206	3.9779	5.2711	4.5130	5.2164	6.3692
1.5	CPT	–	2.7369	4.2266	6.7412	6.7002	8.0870	10.4502	12.6954	14.0476	16.3364
	FOPT	0.1	2.5259	3.7994	5.8304	5.7375	6.7906	8.5182	9.9966	10.8951	12.3770
		0.2	2.1206	3.0735	4.4808	4.3220	5.0470	6.1761	6.9575	7.5331	8.4519
		0.3	1.7499	2.4727	3.4936	3.3156	3.8625	4.6768	5.1638	5.5813	6.2328
		0.4	1.4612	2.0314	2.8232	2.6483	3.0881	3.7215	4.0739	4.3940	4.8944
	HOPT	0.1	2.5297	3.8072	5.8469	5.7577	6.8173	8.5566	10.0559	10.9628	12.4587
		0.2	2.1383	3.1049	4.5401	4.3953	5.1342	6.2898	7.1279	7.7167	8.6600
		0.3	1.7835	2.5284	3.5911	3.4322	3.9968	4.8466	5.4020	5.8387	6.5234
		0.4	1.5084	2.1067	2.9474	2.7926	3.2527	3.9269	4.3512	4.6685	5.2369
2	CPT	–	2.4906	3.2254	4.5370	6.4830	7.2020	8.4382	12.4877	13.2076	14.4258
	FOPT	0.1	2.3098	2.9528	4.0725	5.5710	6.1264	7.0664	9.8584	10.3440	11.1571
		0.2	1.9500	2.4534	3.2912	4.2049	4.5988	5.2465	6.8685	7.1861	7.7090
		0.3	1.6128	2.0130	2.6505	3.2252	3.5329	4.0197	5.0989	5.3333	5.7136
		0.4	1.3481	1.6763	2.1826	2.5748	2.8294	3.2188	4.0233	4.2041	4.4994
	HOPT	0.1	2.3131	2.9577	4.0804	5.5901	6.1487	7.0939	9.9163	10.4061	11.2259
		0.2	1.9657	2.4744	3.3226	4.2759	4.6757	5.3339	7.0366	7.3596	7.8923
		0.3	1.6433	2.0516	2.7058	3.3389	3.6530	4.1531	5.3332	5.5751	5.9694
		0.4	1.3911	1.7296	2.2568	2.7154	2.9773	3.3823	4.2945	4.4700	4.8400

5.1. Natural frequencies of thick plates

The free vibrations of rectangular thick plates are investigated by the proposed above method. Nine frequency factors are obtained for each case based on the three plate theories (CPT, FOPT, HOPT). In all calculations Poisson's ratio v is taken as 0.3. For the FOPT solutions the shear correction factor $k = 5/6$ is adopted. For convenience of notation, the plates are described by a symbolism defining the boundary conditions at their edges starting from $x = 0$ and $x = L_x$, $y = 0$, $y = L_y$, consequently. For example, CCFS denotes a plate with clamped edges at $x = 0$ and $x = L_x$, free at $y = 0$ and simply supported at $y = L_y$. The frequencies are expressed in terms of the dimensionless factor $\lambda = \omega L_y^2/\pi^2(\rho h/D)^{1/2}$. The results obtained by the three theories are presented in table form for the different configurations of the rectangular plates. For each case of the boundary conditions the following properties are considered: aspect ratios $L_x/L_y = 1.0$, 1.5, 2.0 and thickness–width ratios $h/L_y = 0.1$, 0.2, 0.3, 0.4. Note that ratios $h/L_y = 0.4$ does not really ascribe to a plate, but we use it for comparison and confirmation of the obtained results. The mode shapes of vibration are defined by m and n, where these integers indicate the number of half waves in the x- and y-directions, respectively.

5.1.1. SSSS plates

The natural frequency factors λ for the SSSS plates calculated by using the three theories are given in Table 1. The frequencies decrease with an increasing of the thickness–width ratio (h/L_y) for constant values of L_x/L_y. It is seen that this effect is more pronounced for higher modes. Such behavior is due to the

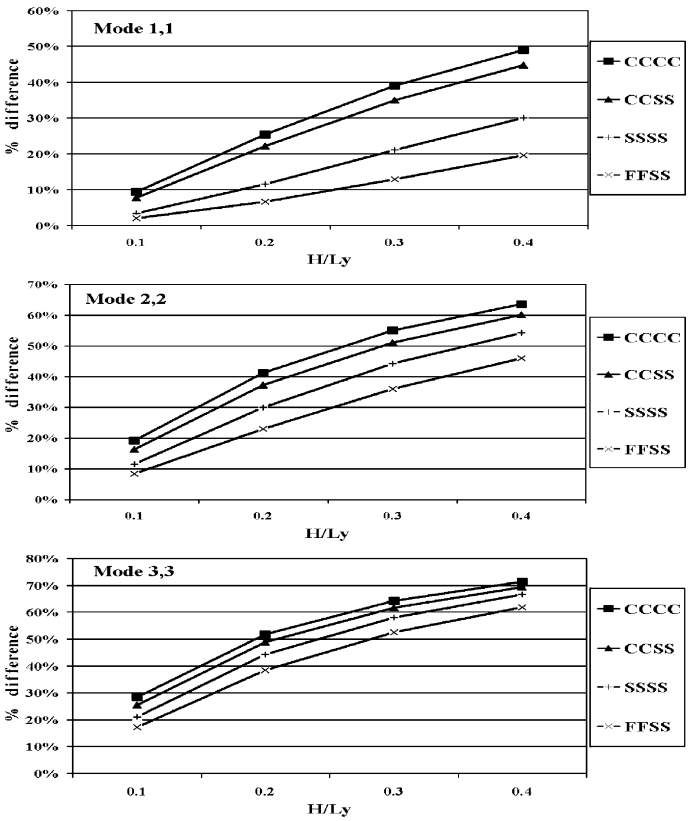

Fig. 4. Comparison of normalized frequency for square plates: % difference CPT to HOPT.

influence of rotary inertia and shear deformations. Also, the discrepancy between the CPT results and the higher theories (HOPT, FOPT) becomes more significant because that CPT does not take into account the additional flexibility due to the shear stresses. The differences between the results obtained by CPT and HOPT for the plates with constant thickness are presented in Fig. 2.

From these figures and tables the influence of the aspect ratio L_x/L_y may be studied too. It may be observed that the frequency factors decrease with an increasing of the aspect ratio L_x/L_y; moreover the discrepancy between the theories decreases as well. This effect ascribes to more flexibility of the longer plates.

The comparison of the HOPT and FOPT results for the square plate is shown in Fig. 3.

It is seen that the difference between the results of these theories is neglected in the cases of lower thickness–width ratios and exceeds the 1% only in the cases of relatively thick plates ($h/L_y = 0.3$, 0.4) for the higher modes (two and more half waves).

Note that the values of the frequency factors obtained based on HOPT are greater than the FOPT results. There are a number of reasons for this effect:

- FOPT needs a shear correction factor to compensate the discrepancy between the assumed constant distributions of the transverse shear strains and its true parabolic variation. On the other hand HOPT require no corrections and as a result the disparity between the results appears.
- The assumed HOPT displacements, which are generally smaller than the FOPT displacements, and the additional high order shear and moment in HOPT lead to higher rigidity of the plate. Thus, the more flexible FOPT scheme results in the smaller values of the natural frequency.

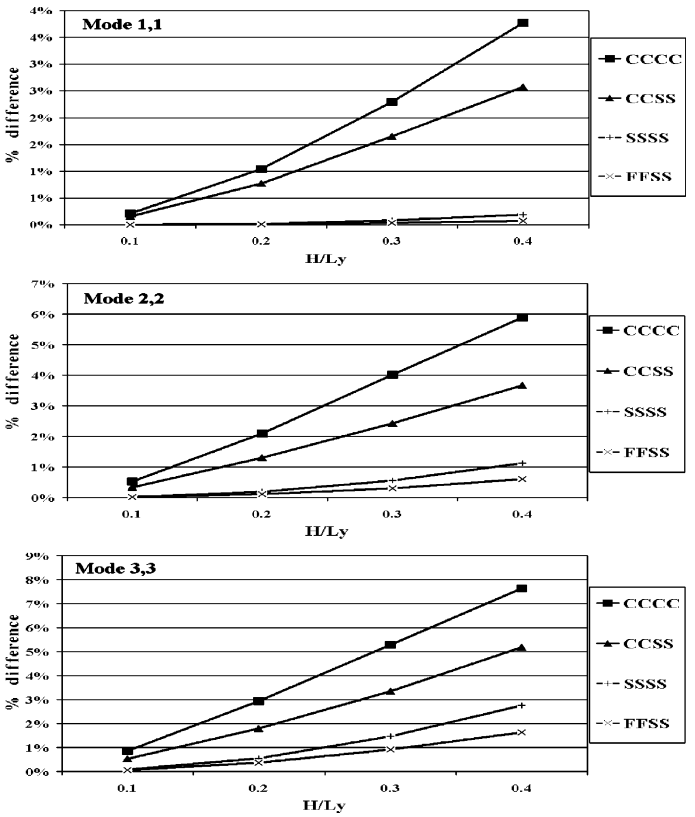

Fig. 5. Comparison of normalized frequency for square plates: % difference FOPT to HOPT.

Comparisons of the results with existing solutions are given in Table 2. The results based on FOPT formulation are compared with those obtained using Navier method by Reddy and Phan (1985) and Rayleigh–Ritz method by Liew et al. (1993b); $k = 0.82305$ is used for these cases. Similar or more precise results are achieved for every case. The comparison for HOPT results is made with Navier solutions of Reddy and Phan (1985) and Matsunga (1994), and good agreement has been achieved. The attained accuracy is also confirmed by comparing our results to the 3-D solution of Liew et al. (1993a).

5.1.2. SSFF plates

The dimensionless values of natural frequency for SSFF plates are compared with those obtained by Liew et al. (1993b) in Table 3. Also, this table shows the similarity of the present HOPT results with the 3-D solution for SSFF plate of Liew et al. (1993a). Total agreement has been found in all the cases, as again this is a separable case.

5.1.3. CCCC plates

The dimensionless values of natural frequencies for clamped rectangular plates are given in Table 4. Comparison with the results for the SSSS plates shows that the frequency factors increase with higher constraints (from simply supported to fully clamped). In order to study the boundary effect, the difference between CPT and HOPT solutions are shown for several frequencies in Fig. 4.

Table 5
Frequency factor λ for CFFF plates

L_x/L_y	Theory	h/L_y	Mode								
			1,1	2,1	3,1	1,2	2,2	3,2	1,3	2,3	3,3
1	CPT	–	0.3556	2.2212	6.2186	0.8668	3.1752	7.1760	2.7474	5.5366	9.8979
	FOPT	0.1	0.3516	2.0946	5.4882	0.8222	2.9001	6.1961	2.5774	4.8598	8.1909
		0.2	0.3418	1.8222	4.3136	0.7501	2.4526	4.7969	2.2816	3.9235	6.1386
		0.3	0.3283	1.5386	3.4051	0.6704	2.0470	3.7651	1.9833	3.1896	4.7613
		0.4	0.3126	1.2967	2.7662	0.5944	1.7296	3.0431	1.7284	2.6587	3.8384
	HOPT	0.1	0.3516	2.0961	5.4981	0.8226	2.9032	6.2089	2.5786	4.8672	8.2119
		0.2	0.3420	1.8307	4.3555	0.7522	2.4668	4.8465	2.2836	3.9512	6.2096
		0.3	0.3288	1.5573	3.4757	0.6751	2.0744	3.8456	1.9909	3.2406	4.8735
		0.4	0.3136	1.3247	2.8527	0.6025	1.7674	3.1327	1.7368	2.7309	3.9568
1.5	CPT	–	0.1580	0.9850	2.7571	0.5266	1.7849	3.6476	2.4730	3.8588	6.0467
	FOPT	0.1	0.1570	0.9577	2.5931	0.5039	1.6767	3.3360	2.3551	3.5136	5.3054
		0.2	0.1546	0.8907	2.2523	0.4677	1.4976	2.8170	2.1208	2.9804	4.2643
		0.3	0.1513	0.8065	1.9102	0.4260	1.3126	2.3494	1.8720	2.5061	3.4487
		0.4	0.1473	0.7212	1.6265	0.3838	1.1502	1.9847	1.6447	2.1326	2.8592
	HOPT	0.1	0.1570	0.9579	2.5946	0.5041	1.6777	3.3389	2.3555	3.5162	5.3119
		0.2	0.1546	0.8921	2.2608	0.4685	1.5019	2.8304	2.1225	2.9908	4.2898
		0.3	0.1514	0.8102	1.9287	0.4279	1.3219	2.3759	1.8737	2.5276	3.4983
		0.4	0.1475	0.7279	1.6542	0.3871	1.1651	2.0226	1.6479	2.1657	2.9365
2	CPT	–	0.0888	0.5530	1.5473	0.3756	1.2266	2.3605	2.3795	3.2010	4.5538
	FOPT	0.1	0.0884	0.5438	1.4919	0.3603	1.1651	2.2072	2.2790	2.9689	4.1029
		0.2	0.0875	0.5202	1.3630	0.3372	1.0654	1.9449	2.0651	2.5834	3.4217
		0.3	0.0862	0.4879	1.2126	0.3101	0.9558	1.6821	1.8312	2.2153	2.8367
		0.4	0.0848	0.4520	1.0710	0.2818	0.8525	1.4588	1.6154	1.9110	2.3869
	HOPT	0.1	0.0884	0.5438	1.4922	0.3604	1.1656	2.2084	2.2788	2.9703	4.1060
		0.2	0.0875	0.5206	1.3655	0.3377	1.0674	1.9504	2.0661	2.5887	3.4342
		0.3	0.0863	0.4890	1.2187	0.3111	0.9603	1.6939	1.8314	2.2266	2.8627
		0.4	0.0848	0.4541	1.0814	0.2836	0.8602	1.4774	1.6243	1.9255	2.4243

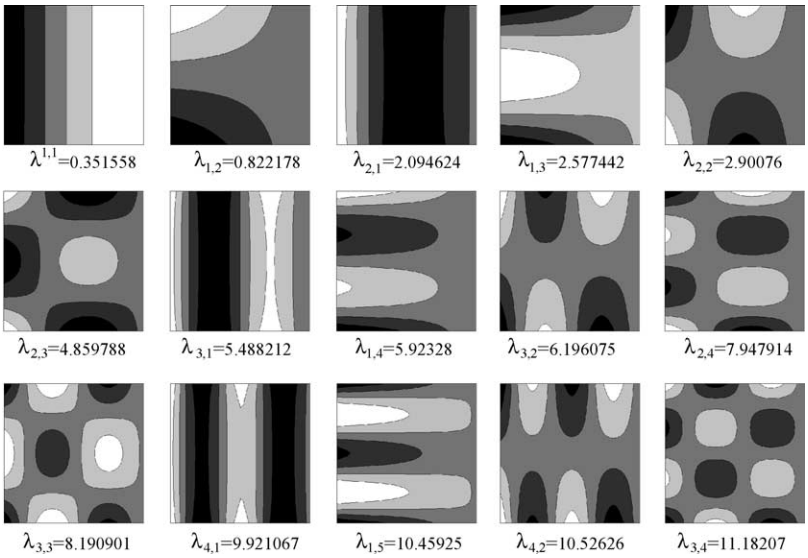

Fig. 6. Free vibration modes for CFFF square plate: $h_0/L_y = 0.1$: HOPT solution.

Table 6
Comparison of the buckling load factors for SSSS plate ($v = 0.3$)

L_x/L_y	Theory	h/L_y	Work	Buckling load		
				P_x	$P_x + P_y$	P_y
1	FOPT	0.1	Present	3.7865	1.8932	3.7865
			Reddy and Phan (1985)	3.7864	–	3.7864
			Wang et al. (1994), Kitipornchai et al. (1993)	3.7865	1.8932	–
		0.2	Present	3.2637	1.6319	3.2637
			Reddy and Phan (1985)	3.2636	–	3.2636
			Wang et al. (1994), Kitipornchai et al. (1993)	3.2637	1.6319	–
	HOPT	0.1	Present	3.7866	1.8933	3.7866
			Reddy and Phan (1985)	3.7865	–	3.7865
		0.2	Present	3.2653	1.6327	3.2653
			Reddy and Phan (1985)	3.2653	–	3.2653
1.5	FOPT	0.1	Present	4.0250	1.3879	2.0048
			Wang et al. (1994), Kitipornchai et al. (1993)	4.0250	1.3879	–
		0.2	Present	3.3048	1.2421	1.7941
			Wang et al. (1994), Kitipornchai et al. (1993)	3.3048	1.2421	–
2	FOPT	0.1	Present	3.7865	1.2074	1.5093
			Wang et al. (1994), Kitipornchai et al. (1993)	3.7865	1.2074	1.5093
		0.2	Present	3.2637	1.0955	1.3694
			Wang et al. (1994), Kitipornchai et al. (1993)	3.2637	1.0955	1.3694
		0.3	Present	2.5726	0.9490	1.1862
			Wang et al. (1994), Kitipornchai et al. (1993)		–	1.1862
		0.4	Present	1.9034	0.7992	0.9991
			Wang et al. (1994), Kitipornchai et al. (1993)	–	–	0.9991

From Fig. 4, one can find that the effect of the thickness ratio on the difference between the theories increases with the stiffening of the boundary constraints of the plates. Thus, the thickness ratio of fully clamped plates has the biggest effect on the natural frequencies. Moreover, it is shown that the discrepancy between the theories increases with the increase in the frequency order. The boundary effect on the difference between HOPT and FOPT is shown in Fig. 5.

It is seen that the discrepancy between the shear deformation theories is most pronounced for the fully clamped plates and decreases with decreasing of boundary constrains.

5.1.4. CFFF plates

The dimensionless values of natural frequencies for cantilevered rectangular plates are given in Table 5. The first 15 mode shapes for a square cantilevered plate with thickness–width ratio $h_0/L_y = 0.1$ are shown in Fig. 6.

5.2. Buckling of thick plates

The stability of rectangular thick plates is studied using the proposed method. Two types of the buckling load are considered, namely the uniform load applied on parallel edges in one direction and

Table 7
Dimensionless buckling loads and modes for SSSS plates

L_x/L_y	Theory	h/L_y	Buckling load and mode						Theories	% difference		
			P_x		$P_x + P_y$		P_y			P_x	$P_x + P_y$	P_y
1	CPT	–	4.0000	1,1	2.0000	1,1	4.0000	1,1				
	FOPT	0.1	3.7865	1,1	1.8932	1,1	3.7865	1,1	HOPT–FOPT	0.00	0.00	0.00
		0.2	3.2637	1,1	1.6319	1,1	3.2637	1,1		0.05	0.05	0.05
		0.3	2.6533	1,1	1.3266	1,1	2.6533	1,1		0.20	0.20	0.20
		0.4	1.9196	1,2	1.0513	1,1	1.9196	2,1		1.81	0.50	1.81
	HOPT	0.1	3.7866	1,1	1.8933	1,1	3.7866	1,1	CPT–HOPT	5.34	5.34	5.34
		0.2	3.2653	1,1	1.6327	1,1	3.2653	1,1		18.37	18.37	18.37
		0.3	2.6586	1,1	1.3293	1,1	2.6586	1,1		33.54	33.53	33.54
		0.4	1.9550	1,2	1.0567	1,1	1.9550	2,1		51.12	47.17	51.12
1.5	CPT	–	4.3403	2,1	1.4444	1,1	2.0864	1,1				
	FOPT	0.1	4.0250	2,1	1.3879	1,1	2.0048	1,1	HOPT–FOPT	0.01	0.00	0.00
		0.2	3.3048	2,1	1.2421	1,1	1.7941	1,1		0.09	0.03	0.03
		0.3	2.5457	2,1	1.0570	1,1	1.5267	1,1		0.34	0.12	0.12
		0.4	1.9196	3,1	0.8745	1,1	1.2632	1,1		1.16	0.30	0.30
	HOPT	0.1	4.0253	2,1	1.3879	1,1	2.0048	1,1	CPT–HOPT	7.26	3.91	3.91
		0.2	3.3077	2,1	1.2424	1,1	1.7946	1,1		23.79	13.99	13.99
		0.3	2.5545	2,1	1.0582	1,1	1.5285	1,1		41.15	26.74	26.74
		0.4	1.9421	2,1	0.8772	1,1	1.2670	1,1		55.25	39.27	39.27
2	CPT	–	4.0000	2,1	1.2500	1,1	1.5625	1,1				
	FOPT	0.1	3.7865	2,1	1.2074	1,1	1.5093	1,1	HOPT–FOPT	0.00	0.00	0.00
		0.2	3.2637	2,1	1.0955	1,1	1.3694	1,1		0.05	0.02	0.02
		0.3	2.5726	3,1	0.9490	1,1	1.1862	1,1		0.44	0.09	0.09
		0.4	1.9034	3,1	0.7992	1,1	0.9991	1,1		1.02	0.24	0.24
	HOPT	0.1	3.7866	2,1	1.2075	1,1	1.5093	1,1	CPT–HOPT	5.34	3.40	3.40
		0.2	3.2654	2,1	1.0958	1,1	1.3697	1,1		18.37	12.34	12.34
		0.3	2.5839	3,1	0.9498	1,1	1.1873	1,1		35.40	24.01	24.01
		0.4	1.9230	3,1	0.8012	1,1	1.0015	1,1		51.93	35.91	35.91

uniform load applied on all edges. The symbolism and parameters of computation are the same as described in the part of the free vibration. The buckling load P is expressed as a dimensionless value, $\overline{P} = NL_y^2/\pi^2 D$.

5.2.1. SSSS plates

The comparisons of the dimensionless buckling loads for SSSS plates with the solutions of Reddy and Phan (1985) by HOPT and FOPT, Wang et al. (1994) and Kitipornchai et al. (1993) by FOPT are given in Table 6. Total agreement is achieved for all the results.

The values of the normalized buckling loads and shapes for simply supported rectangular plates are given in Table 7. It is seen that the buckling load decreases with an increase in the thickness–width ratio. Also, the discrepancy between the shear deformation and classical theories becomes more appreciable. The first order theory is in fairly good agreement with the higher order theory and the maximum difference between the values of buckling loads predicted by FOPT and HOPT is less than 2%. Moreover, it can be observed that the shear stresses not only reduce the values of the buckling load but also cause changes in the buckling shapes. To examine this point, more detailed computations have been performed for very small steps of thickness–width ratio, and are summarized in Table 8.

From the table it can be observed that the two shear deformation theories result in different shapes for the same thickness–width ratio ($h_0/L_y = 0.33$) in the case of square plate and in the case of rectangular plates FOPT leads to the change of modes for the smaller thickness–width ratios than HOPT (see Fig. 7).

5.2.2. SSFF plates

Full agreement of the obtained results for SSFF plates with the solution of Kitipornchai et al. (1993) by Rayleigh–Ritz method and Liew et al. (1996) by Levy method is shown in Table 9.

Table 8
Comparison of buckling shapes for SSSS plates

L_x/L_y	h/L_y	Buckling load P_x and mode			
		FOPT		HOPT	
1	0.31	2.5941	1,1	2.5999	1,1
	0.32	2.5356	1,1	2.5419	1,1
	0.33	2.4651	**2,1**	2.4849	1,1
	0.34	2.3765	2,1	2.4051	**2,1**
	0.35	2.2917	2,1	2.3214	2,1
	0.36	2.2106	2,1	2.2414	2,1
	0.37	2.1330	2,1	2.1650	2,1
	0.38	2.0587	2,1	2.0919	2,1
	0.39	1.9876	2,1	2.0219	2,1
2	0.21	3.2033	2,1	3.2043	2,1
	0.22	3.1423	2,1	3.1473	2,1
	0.23	3.0808	2,1	3.0903	2,1
	0.24	3.0192	2,1	3.0397	2,1
	0.25	2.9575	2,1	2.9637	2,1
	0.26	2.8959	2,1	3.2186	2,1
	0.27	2.8142	**3,1**	2.8370	2,1
	0.28	2.7317	3,1	2.7610	2,1
	0.29	2.6511	3,1	2.6850	2,1
	0.3	2.5726	3,1	2.5869	**3,1**

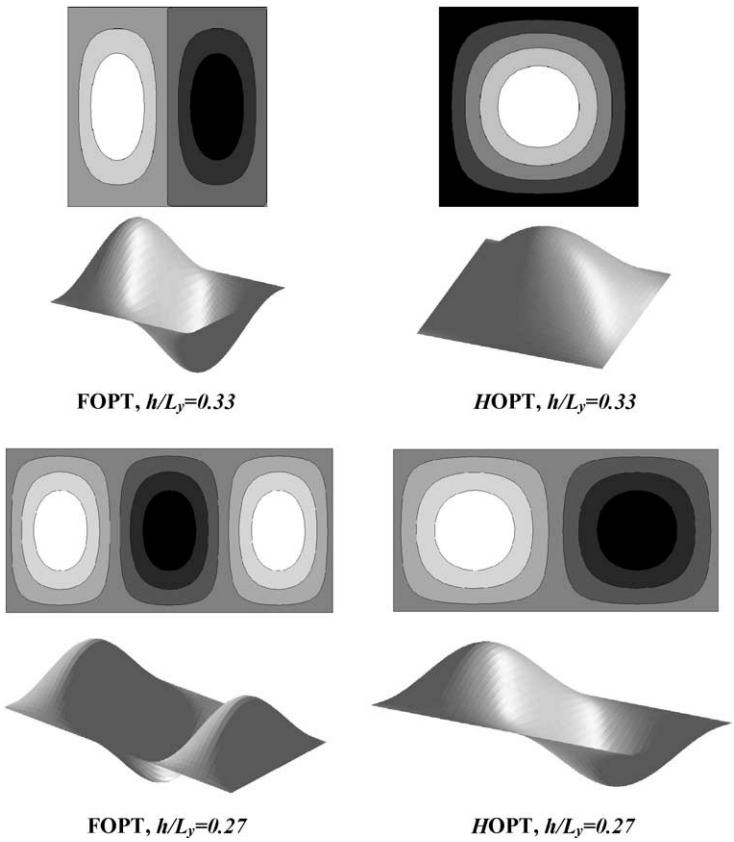

Fig. 7. Comparison of buckling shapes for SSSS plates, uniformly compressed in x-direction.

5.2.3. CCCC plates

The comparison of buckling load factors for fully clamped rectangular plate with the solutions of Wang et al. (1994) and Kitipornchai et al. (1993) are given in Table 10. Although the solution of the fully clamped plates is not separable, the extended Kantorovich method leads to very good approximation of the first eigenvalue and there are only small differences between the results (up to 0.4%). The dimensionless buckling loads and shapes for CCCC rectangular plates are represented in Table 11. It is seen that the discrepancy between the theories increases with an increase in the boundary constraints both in the values of buckling loads and in the shapes. In order to study the influence of the thickness–width ratio on the stability of the shear deformable plates, the normalized buckling loads for square plates are shown in Fig. 8 for different boundary conditions. From the figure, one can find that the effect of the thickness–width ratio increases with the increase of the boundary constraint of plates.

5.2.4. CFFF plates

The dimensionless values of buckling loads for cantilevered rectangular plates uniformly compressed in the x-direction and in both directions are given in Table 12. It can be observed that the difference between the theories is very small; moreover all of them lead to the same buckling shapes. This effect is due to the higher flexibility of cantilevered plate. Note that for this case Mode 1, 1 symbolizes a quarter of a wave in the x-direction and wide curve in the y-direction.

Table 9
Comparison of the buckling loads factors for SSFF plate ($v = 0.3$, $k = 5/6$)

L_x/L_y	Theory	h/L_y	Work	Buckling load		
				P_x	$P_x + P_y$	P_y
1	FOPT	0.05	Present	0.9433	0.9208	1.9469
			Liew et al. (1996)		0.9207	1.9464
		0.1	Present	0.9222	0.8977	1.8234
			Liew et al. (1996)		0.8977	1.8233
			Kitipornchai et al. (1993)	0.9222		
		0.15	Present	0.8908	0.8650	1.6839
			Liew et al. (1996)		0.8650	1.6839
		0.2	Present	0.8512	0.8248	1.5372
			Kitipornchai et al. (1993)	0.8512		
1.5	FOPT	0.1	Present	0.4102	0.4026	0.7025
			Kitipornchai et al. (1993)	0.4102		
		0.2	Present	0.3949	0.3869	0.6300
			Kitipornchai et al. (1993)	0.3949		
2	FOPT	0.1	Present	0.2300	0.2270	0.3674
			Liew et al. (1996)		0.2270	0.3674
			Kitipornchai et al. (1993)	0.2300		
		0.2	Present	0.2250	0.2219	0.3354
			Liew et al. (1996)		0.2219	0.3354
			Kitipornchai et al. (1993)	0.2250		
		0.3	Present	0.2175	0.2144	0.3020
			Liew et al. (1996)		0.2144	0.3020

Table 10
Comparison of the buckling load factors for CCCC plate, FOPT solution ($v = 0.3$, $k = 5/6$)

L_x/L_y	h_0/L_y	Work	Buckling load	
			P_x	$P_x + P_y$
1	0.1	Present	8.3231	4.5648
		Kitipornchai et al. (1993)	8.2917	
		Wang et al. (1994)		4.5479
	0.2	Present	5.3293	3.2529
		Kitipornchai et al. (1993)	5.3156	
		Wang et al. (1994)		3.2399
1.5	0.1	Present	6.9748	3.6564
		Kitipornchai et al. (1993)	6.9608	
		Wang et al. (1994)		3.6466
	0.2	Present	4.7225	2.7460
		Kitipornchai et al. (1993)	4.7153	
		Wang et al. (1994)		2.7367
2	0.1	Present	6.5819	3.5014
		Kitipornchai et al. (1993)	6.5736	
		Wang et al. (1994)		3.4953
	0.2	Present	4.5065	2.6524
		Kitipornchai et al. (1993)	4.5026	
		Wang et al. (1994)		2.6458

Table 11
Dimensionless buckling loads and modes for CCCC plates

L_x/L_y	Theory	h_0/L_y	Buckling load and mode					
			P_x		$P_x + P_y$		P_y	
1	CPT	–	10.0968	1,1	5.3148	1,1	10.0968	1,1
	FOPT	0.1	8.3231	1,1	4.5648	1,1	8.3231	1,1
		0.2	5.3293	3,1	3.2529	1,1	5.3293	1,3
		0.3	3.2222	3,1	2.2183	1,1	3.2222	1,3
		0.4	2.0547	3,1	1.5395	1,1	2.0547	1,3
	HOPT	0.1	8.3513	1,1	4.5667	1,1	8.3513	1,1
		0.2	5.4071	2,1	3.2640	1,1	5.4072	1,2
		0.3	3.3306	2,1	2.2413	1,1	3.3306	1,2
		0.4	2.2033	2,1	1.5727	1,1	2.2033	1,2
1.5	CPT	–	8.3609	2,1	4.1278	1,1	5.8309	1,1
	FOPT	0.1	6.9748	2,1	3.6564	1,1	5.1349	1,1
		0.2	4.7225	4,1	2.7460	1,1	3.7996	1,1
		0.3	3.0573	4,1	1.9558	1,1	2.6387	1,3
		0.4	2.0189	4,1	1.4009	1,1	1.8208	1,3
	HOPT	0.1	6.9934	2,1	3.6575	1,1	5.1389	1,1
		0.2	4.7891	4,1	2.7532	1,1	3.8222	1,1
		0.3	3.1494	3,1	1.9723	1,1	2.6911	1,3
		0.4	2.1285	3,1	1.4257	1,1	1.9066	1,3
2	CPT	–	7.8739	3,1	3.9275	1,1	4.8369	1,1
	FOPT	0.1	6.5819	3,1	3.5014	1,1	4.3091	1,1
		0.2	4.5065	5,1	2.6524	3,1	3.2600	1,1
		0.3	2.9783	5,1	1.8983	3,1	2.3244	1,1
		0.4	2.0011	5,1	1.3638	3,.1	1.6555	1,3
	HOPT	0.1	6.5986	3,1	3.5023	1,1	4.3106	1,1
		0.2	4.5848	3,1	2.6590	1,1	3.2696	1,1
		0.3	3.0545	4,1	1.9143	3,1	2.3475	1,1
		0.4	2.0999	4,1	1.3885	3,1	1.6938	1,1

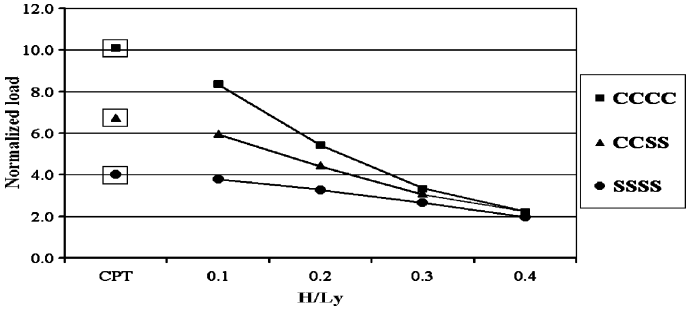

Fig. 8. Dimensionless buckling loads for square plates; HOPT and CPT results.

6. Conclusions

The natural frequencies and buckling loads for rectangular thick plates with different boundary conditions have been investigated by using the extended Kantorovich method. The two shear deformation

Table 12
Dimensionless buckling loads and modes for CFFF plates

L_x/L_y	Theory	h_0/L_y	Buckling load and mode			
			P_x		$P_x + P_y$	
1	CPT	–	0.2475	1,1	0.2472	1,1
	FOPT	0.1	0.2449	1,1	0.2445	1,1
		0.2	0.2378	1,1	0.2375	1,1
		0.3	0.2283	1,1	0.2280	1,1
		0.4	0.2171	1,1	0.2168	1,1
	HOPT	0.1	0.2448	1,1	0.2444	1,1
		0.2	0.2378	1,1	0.2375	1,1
		0.3	0.2283	1,1	0.2279	1,1
		0.4	0.2171	1,1	0.2167	1,1
1.5	CPT	–	0.1097	1,1	0.1096	1,1
	FOPT	0.1	0.1090	1,1	0.1089	1,1
		0.2	0.1072	1,1	0.1071	1,1
		0.3	0.1047	1,1	0.1046	1,1
		0.4	0.1018	1,1	0.1017	1,1
	HOPT	0.1	0.1090	1,1	0.1089	1,1
		0.2	0.1071	1,1	0.1071	1,1
		0.3	0.1046	1,1	0.1045	1,1
		0.4	0.1018	1,1	0.1017	1,1
2	CPT	–	0.0616	1,1	0.0616	1,1
	FOPT	0.1	0.0614	1,1	0.0613	1,1
		0.2	0.0606	1,1	0.0605	1,1
		0.3	0.0595	1,1	0.0595	1,1
		0.4	0.0584	1,1	0.0583	1,1
	HOPT	0.1	0.0616	1,1	0.0616	1,1
		0.2	0.0605	1,1	0.0605	1,1
		0.3	0.0595	1,1	0.0595	1,1
		0.4	0.0584	1,1	0.0583	1,1

theories, in which the effects of both transverse shear stresses and rotary inertia are accounted for, have been applied to the plate's analysis. The large number of numerical examples demonstrates the applicability and versatility of the present method. The advantages of the proposed method are as follows:

- The shape functions are exact solutions for the system of the differential equations of motion and they are derived automatically. As a result, the solution for stability and free vibrations problem is the highly accurate solution (depending only on the accuracy of the numerical calculations), as the only approximation is assuming one term separable solution.
- The exact solution is guaranteed when at least two parallel edges of the plate are simply supported and the problem is separable (Levy and Navier cases). For other cases, it has been found that the proposed simplest one terms separation of variables, Eqs. (3a)–(3c), leads to highly accurate solutions.

The results of the vibration and stability analysis of thick plates can be summarized as follows:

- The factors of the natural frequencies and the buckling loads for rectangular thick plates are dependent on the thickness–width, side-aspect ratios and boundary conditions.

- The natural frequency factors decrease and the discrepancy between results obtained by the three theories (CPT, HOPT, FOPT) increases with an increasing in the thickness of plate; this effect is more significant for higher modes in the cases of lower thickness–width ratios and for all modes in the cases of thicker plates. Note that difference between the two shear deformation theories is negligible for the lower modes.
- The normalized natural frequencies and also the discrepancy between the theories decrease with a decrease in the rigidity of plate, such as greater aspect ratio or less restraining boundary.
- The values of buckling loads factors decrease while the number of half waves in buckling shape increases with an increase in the thickness–width ratio, and the discrepancy between the shear deformation and classical theories becomes more appreciable. The first order theory is in fairly good agreement with the higher order theory, but sometimes there is difference in the buckling shapes.

Acknowledgment

The support for this research to the first author by the Technion Israel Institute of Technology is gratefully acknowledged.

References

Cheung, Y.K., Zhou, D., 2000. Vibrations of moderately thick rectangular plates in terms of a set of static Timoshenko beam functions. Computers & Structures 78 (6), 757–768.

Dawe, D.J., Roufael, O.L., 1982. Buckling of rectangular mindlin plates. Computer & Structures 15 (4), 461–471.

Doong, J.L., 1987. Vibration and stability of an initially stressed thick plate according to a higher order deformation theory. Journal of Sound and Vibration 113 (3), 425–440.

Eisenberger, M., 1991. Buckling loads for variable cross-section members with variable axial forces. International Journal of Solids and Structures 27 (2), 135–143.

Eisenberger, M., 1995. Dynamic stiffness matrix for variable cross-section Timoshenko beams. Communications in Numerical Methods in Engineering 11, 507–513.

Eisenberger, M., 2003. An exact high order beam element. Computers & Structures 81, 147–152.

Eisenberger, M., Alexandrov, A., 2003. Buckling loads of variable thickness thin isotropic plates. Thin-Walled Structures 41 (9), 871–889.

Hanna, N.F., Leissa, A.W., 1994. A higher order shear deformation theory for the vibration of thick plates. Journal of Sound and Vibration 170 (4), 545–555.

Kerr, A.D., 1969. An extended Kantorovich method for the solution of eigenvalue problem. International Journal of Solids and Structures 5, 559–572.

Kitipornchai, S., Xiang, Y., Wang, C.M., Liew, K.M., 1993. Buckling of thick skew plates. International Journal for Numerical Method in Engineering 36, 1299–1310.

Liew, K.M., Hung, K.C., Lim, M.K., 1993a. A continuum three-dimensional vibration analysis of thick rectangular plates. International Journal of Solids and Structures 30 (24), 3357–3379.

Liew, K.M., Xiang, Y., Kitipornchai, S., Wang, C.M., 1993b. Vibration of thick skew plates based on mindlin shear deformation plate theory. Journal of Sound and Vibration 165 (1), 39–69.

Liew, K.M., Xiang, Y., Kitipornchai, S., 1995. Research on thick plate vibration. A literature survey. Journal of Sound and Vibration 180 (1), 163–176.

Liew, K.M., Xiang, Y., Kitipornchai, S., 1996. Analytical buckling solutions for mindlin plates involving free edges. International Journal of Mechanical Sciences 38 (10), 1127–1138.

Liew, K.M., Wang, C.M., Xiang, Y., Kitipornchai, S., 1998. Vibration of Mindlin Plates. Elsevier, Amsterdam.

Matsunga, H., 1994. Free vibration and stability of thick elastic plates subjected to in-plane forces. Journal of Solids and Structures 31 (22), 3113–3124.

Mizusawa, T., 1993. Vibration of rectangular mindlin plates by the spline strip method. Journal of Sound and Vibration 163 (2), 193–205.

Reddy, J.N., 1999. Theory and Analysis of Elastic Plates. Taylor & Francis, Philadelphia.
Reddy, J.N., Phan, N.D., 1985. Stability and vibration of isotropic, orthotropic and laminated plates according to a higher-order shear deformation theory. Journal of Sound and Vibration 98 (2), 157–170.
Roufael, O.L., Dawe, D.J., 1980. Vibration analysis of rectangular mindlin plates by the finite strip method. Computer & Structures 12, 833–842.
Wang, C.M., Xiang, Y., Kitipornchai, S., Liew, K.M., 1994. Buckling solutions for mindlin plates of various shapes. Engineering Structures 16 (2), 119–127.
Wang, C.M., Reddy, J.N., Lee, K.H., 2000. Shear Deformable Beams and Plates. Relationships with Classical Solution. Elsevier, Amsterdam.
Yuan, S., Jin, Y., 1998. Computation of elastic buckling loads of rectangular thin plates using the extended Kantorovich method. Computers & Structures 66 (6), 861–867.
Zenkour, A.M., 2001. Buckling and free vibration of elastic plates using simple and mixed shear deformation theories. ACTA Mechanica 145, 183–197.